Gamma-ray burst from a dust-rich region with a molecular gas shortage

B. Hatsukade[1], K. Ohta[2], A. Endo[3], K. Nakanishi[1,4,5], Y. Tamura[6], T. Hashimoto[1], & K. Kohno[6,7]

[1]National Astronomical Observatory of Japan, 2-21-1 Osawa, Mitaka, Tokyo 181-8588, Japan

[2]Department of Astronomy, Kyoto University, Kyoto 606-8502, Japan

[3]Kavli Institute of NanoScience, Faculty of Applied Sciences, Delft University of Technology, Lorentzweg 1, 2628 CJ Delft, The Netherlands

[4]Joint ALMA Observatory, Alonso de Córdova 3107, Vitacura, Santiago 763 0355, Chile

[5]The Graduate University for Advanced Studies (Sokendai), 2-21-1 Osawa, Mitaka, Tokyo 181-8588, Japan

[6]Institute of Astronomy, University of Tokyo, 2-21-1 Osawa, Mitaka, Tokyo 181-8588, Japan

[7]Research Centre for the Early Universe, University of Tokyo, 7-3-1 Hongo, Bunkyo, Tokyo 113-0033, Japan

Long-duration γ-ray bursts are associated with the explosions of massive stars[1] and are accordingly expected to reside in star-forming regions with molecular gas (the fuel for star formation). Previous searches for carbon monoxide (CO), a tracer of molecular gas, in burst host galaxies did not detect any emission[2,3,4]. Molecules have been detected in absorption in the spectra of γ-ray burst afterglows, and the gas is similar to the translucent or diffuse molecular clouds of the Milky Way[5,6]. Absorption lines probe the interstellar medium only along the sightline, so it is not clear whether they represent the general properties of the regions where the bursts occur. Here we report spatially-resolved observations of CO emission line and millimetre-wavelength continuum emission in two host galaxies. The bursts happened in regions rich with dust, but not particularly rich in molecular gas. The molecular gas-to-dust ratio of <9–14 is significantly lower than in star forming regions of the Milky Way and nearby star-forming galaxies, suggesting that much of the dense gas where stars form has largely been incorporated into stars or dissipated by other massive stars.

We selected the two γ-ray burst (GRB) hosts (GRB 020819B at a redshift of $z = 0.41$ and GRB 051022 at $z = 0.81$) with high star formation rates (SFRs) and high gas metallicity among GRB host galaxies to maximize the possibility of detecting the CO emission line and dust continuum emission. The GRB 020819B host shows an extinction-corrected SFR of ~10–30 $M_\odot$ yr^{-1} (where $M_\odot$ indicates solar mass) derived from ultraviolet (UV) continuum emission, the Hα emission line, and spectral energy (SED) fit with infrared (IR) data[7,8,9]. The SFRs at spatially-resolved positions are also derived from the Hα emission line, which are 10.3 $M_\odot$ yr^{-1} and 23.6 $M_\odot$ yr^{-1} at the nuclear region and at the GRB explosion site, respectively[8]. The host galaxy of GRB 051022 shows an extinction-corrected SFR of ~20–70 $M_\odot$ yr^{-1} derived from UV continuum emission, the [O II] λ3727 emission line, SED fit with IR data, and radio continuum emission[7,9,10,11]. The gas metallicity is measured at the GRB 020819B site, the nuclear region of the GRB 020819B host, and the GRB 051022 host, and they all have (super-)solar metallicity[8,12]. The two GRBs are classified as `dark GRBs'[13,14], whose afterglow is optically dark compared with what is expected from X-ray afterglows[15]. The origin of the dark GRBs is not yet understood well, but a plausible explanation is dust obscuration along the line of sight to GRBs[16,17,18,19].

We conducted observations of the CO emission line and 1.2 mm continuum towards the GRB hosts using the Atacama Large Millimeter/submillimeter Array (ALMA). We observed the redshifted CO(3–2) line for the GRB 020819B host and the CO(4–3) line for the GRB 051022 host. The angular resolution is ~0.8″ × 0.7″ (~4 kpc × 4 kpc) and ~1.0″ × 0.7″ (~8 kpc × 5 kpc) (full-width at half maximum; FWHM) for the GRB 020819B host and the GRB 051022 host, respectively. The GRB 020819B host is spatially-resolved in the observations. The CO emission line is clearly detected at the nuclear region of the GRB 020819B host and the GRB 051022 host (Figs. 1a, d, and 2). While molecular gas has been detected in absorption in the spectra of GRB afterglows[5,6], this is the first case for detecting spatially-resolved molecular gas emission in GRB hosts[2,3,4]. The molecular gas mass estimated from the CO emission is $M_{\rm gas} = 2.4 \times 10^9\ M_\odot$ and $2.1 \times 10^9\ M_\odot$ for the nuclear region of the GRB 020819B host and the GRB 051022 host, respectively (see Methods). The molecular gas mass is comparable to those of local massive spiral galaxies[20], and lower than those of $z \sim 1$–2 normal star-forming galaxies[21] or submillimetre-luminous galaxies (SMGs)[22,23]. The fraction of molecular gas mass to stellar mass[7,24] for the hosts is ~0.1, which is comparable to those of local spiral galaxies[20].

The 1.2 mm continuum emission is also detected in both GRB hosts (Fig. 1b, e). The spatially-resolved continuum map of the GRB 020819B host shows that the emission is significantly detected only at a star-forming region ~3" (16 kpc in projection) away from the nuclear region, where the GRB explosion occurred. The size of the continuum emission deconvolved from the telescope beam is ~1.7 kpc × 1.0 kpc. We regard the continuum emission as dust thermal emission originated in star-forming activity. By assuming that the dust emission is described as a modified blackbody and using the dust temperature and emissivity index derived from fitting, we derive the dust mass of $M_{\rm dust} = 4.8 \times 10^7\ M_\odot$ and $2.9 \times 10^7\ M_\odot$ for the GRB 020819B site and the GRB 051022 host, respectively (see Methods). The far-IR luminosity and SFR are $L_{\rm FIR} = 1.1 \times 10^{11}\ L_\odot$ and SFR = $18\ M_\odot\ {\rm yr}^{-1}$ for the GRB 020819B site, and $L_{\rm FIR} = 1.9 \times 10^{11}\ L_\odot$ and SFR = $32\ M_\odot\ {\rm yr}^{-1}$ for the GRB 051022 host, respectively. The SFRs are comparable to the extinction-corrected SFRs derived from UV and optical observations, suggesting that there is no sign of an extra, optically completely invisible portion of star formation that cannot be recovered by extinction correction.

Of particular interest is that the spatial distributions of molecular gas and dust are clearly different in the GRB 020819B host. The ratio of molecular gas mass to dust mass of the GRB 020819B host is >58–86 and <9–14 (3σ limits with uncertainty from dust mass) at the nuclear region and the GRB site, respectively. The ratio in the GRB site is significantly lower than that of the nuclear region, indicating that the GRB occurred in a particular circumstance within the host. The molecular gas-to-dust ratio at the GRB site is also lower than those of the Milky Way and nearby star-forming galaxies[25], suggesting that the star-forming environment where GRBs occur is different from those in local galaxies. While the correlation between gas-to-dust ratio and metallicity has been observed[20,25], it is unlikely that the large difference between the GRB site and the nuclear region is attributed to the difference in metallicity because both regions have a similar metallicity[8]. The difference of distribution between molecular gas and dust is also seen in the GRB 051022 host and the GRB site seems to be a dust-rich region, although the angular resolution is not good enough to be definitive. The possible reasons for the deficit of molecular gas in the GRB site is that much of the dense gas where stars form has been incorporated into stars, or dissipated by a strong interstellar UV radiation field, which is expected in regions with intense star formation. The lack of molecular gas in optical spectra of GRB afterglows has been reported[26] and a possible explanation is the dissociation of molecules by ambient UV radiation with 10–100 times the Galactic mean value from the star-forming regions where GRB progenitors reside[26,27]. GRB hosts with a mean UV radiation field of 35–350 times the Galactic mean value are actually observed[28]. The molecular gas-to-dust ratio in GRB hosts could be an important indicator for examining the environment where GRBs occur.

The occurrence of GRB 020819B in a dust-rich region supports the idea that the dust extinction is the cause for the darkness of optical afterglow[13,24]. The molecular gas-to-dust ratio in the GRB site is comparable to or lower than nuclear regions of local galaxies (~20–40) (ref. 29) and SMGs (~50) (ref. 30), suggesting the existence of GRBs that could occur in dusty galaxies such as SMGs.

1. Stanek, K. *et al*. Spectroscopic discovery of the supernova 2003dh associated with GRB 030329. *Astrophys. J.* **591**, L17–L20 (2003)

2. Kohno, K. *et al*. Nobeyama Millimeter Array observations of GRB 030329: a decay of afterglow with bumps and molecular gas in the host galaxy. *Publ. Astron. Soc. Japan* **57**, 147–153 (2005)

3. Endo, A. *et al.* A revised estimate of the CO J = 1–0 emission from the host galaxy of GRB 030329 using the Nobeyama Millimeter Array. *Astrophys. J.* **659**, 1431–1437 (2007)

4. Hatsukade, B., Kohno, K., Endo, A., Nakanishi, K., & Ohta, K. CO observations of the host galaxy of GRB 000418 at z = 1.1. *Astrophys. J.* **738**, 33–36 (2011)

5. Prochaska, J. X. *et al.* The first positive detection of molecular gas in a GRB host galaxy. *Astrophys. J.* **691**, L27–L32 (2009)

6. Krühler, T. *et al.* Molecular hydrogen in the damped Lyman α system towards GRB 120815A at z = 2.36. *Astron. Astrophys*. **557**, 18–38 (2013)

7. Savaglio, S., Glazebrook, K., & Le Borgne, D. The galaxy population hosting gamma-ray bursts. *Astrophys. J.* **691**, 182–211 (2009)

8. Levesque, E. M., Kewley, L. J., Graham, J. F., & Fruchter, A. S. A high-metallicity host environment for the long-duration GRB 020819B. *Astrophys. J.* **712**, L26–L30 (2010)

9. Hunt, L. K. *et al.* New light on gamma-ray burst host galaxies with *Herschel*. *Astron. Astrophys.*

arXiv:1402.4006 (2014)

10. Castro-Tirado, A. J. *et al*. The dark nature of GRB 051022 and its host galaxy. *Astron. Astrophys.* **475**, 101–107 (2007)

11. Perley, D. A., & Perley, R. A. Radio constraints on heavily-obscured star-formation within dark gamma-ray burst host galaxies. *Astrophys. J.* **778**, 172–189 (2013)

12. Graham, J. F. *et al*. Unusually high metallicity host of the dark LGRB 051022. *American Institute of Physics Conference Series*, **1133**, 269–271 (2009)

13. Jakobsson, P. *et al*. The radio afterglow and host galaxy of the dark GRB 020819B. *Astrophys. J.* **629**, 45–51 (2005)

14. Rol, E. *et al*. GRB 051022: Physical parameters and extinction of a prototype dark burst. *Astrophys. J.* **669**, 1098–1106 (2007)

15. Jakobsson, P. *et al*. *Swift* identification of dark gamma-ray bursts. *Astrophys. J.* **617**, L21–L24 (2004)

16. Perley, D. A. *et al*. The host galaxies of *Swift* dark gamma-ray bursts: observational constraints on highly obscured and very high redshift GRBs. *Astron. J.* **138**, 1690–1708 (2009)

17. Cenko, S. B. et al. Dark bursts in the Swift Era: The Palomar 60 Inch-Swift Early Optical Afterglow Catalog. *Astrophys. J.* **693**, 1484–1493 (2009)

18. Greiner, J. *et al.* The nature of ``dark'' gamma-ray bursts. *Astron. Astrophys.* **526**, 30–39 (2011)

19. Campana, S. *et al.* The X-ray absorbing column density of a complete sample of bright Swift gamma-ray bursts. *Mon. Not. R. Astron. Soc.* **421**, 1697–1702 (2012)

20. Leroy, A. K. *et al*. Heracles: The HERA CO line extragalactic survey. *Astron. J.* **137**, 4670–4696 (2009)

21. Tacconi, L. J. *et al*. Phibss: Molecular gas content and scaling relations in *z* ~ 1–3 massive, main-sequence star-forming galaxies. *Astrophys. J.* **768**, 74–95, (2013)

22. Bothwell, M. S. *et al*. A survey of molecular gas in luminous sub-millimetre galaxies. *Mon. Not. R. Astron. Soc.* **429**, 3047–3067 (2013)

23. Solomon, P. M., & Vanden Bout, P. A. Molecular gas at high redshift. *Annu. Rev. Astron. Astrophys.* **43**, 677–725 (2005)

24. Küpcü Yoldaş, A., Greiner, J., Klose, S., Krühler, T., & Savaglio, S. Highly extinguished host galaxy of the dark GRB 020819B. *Astron. Astrophys.* **515**, L2–L5 (2010)

25. Draine, B. T. *et al*. Dust masses, PAH abundances, and starlight intensities in the SINGS galaxy sample. *Astrophys. J.* **663**, 866–894 (2007)

26. Tumlinson, J., Prochaska, J. X., Chen, H.-W., Dessauges-Zavadsky, M., & Bloom, J. S. Missing molecular hydrogen and the physical conditions of GRB host galaxies. *Astrophys. J.* **668**, 667–

673 (2007)

27. Whalen, D., Prochaska, J. X., Heger, A., & Tumlinson, J. The molecular hydrogen deficit in gamma-ray burst afterglows. *Astrophys. J.* **682**, 1114–1123 (2008)

28. Chen, H.-W. *et al.* High-redshift starbursting dwarf galaxies revealed by γ-ray burst afterglows. *Astrophys. J.* **691**, 152–174 (2009)

29. Seaquist, E., Yao, L., Dunne, L., & Cameron, H. Revised masses of dust and gas of SCUBA Local Universe Survey far-infrared bright galaxies based on a recent CO survey. *Mon. Not. R. Astron. Soc.*, **349**, 1428–1434 (2004)

30. Kovács, A. *et al.* SHARC-2 350 μm observations of distant submillimeter-selected galaxies. *Astrophys. J.* **650**, 592–603 (2006)

Supplementary Information is available in the online version of the paper.

Acknowledgements

We acknowledge Akiko Kawamura and ALMA staffs for helpful support. We are grateful to Kiyoto Yabe and Akifumi Seko for useful discussions. We thank the editor and referees for helpful comments and suggestions. This research was supported by Research Fellowship for Young Scientists and the Grant-in-Aid for Scientific Research (C) (24540230) from the Japan Society of the Promotion of Science (JSPS). ALMA is a partnership of ESO (representing its member states), NSF (USA) and NINS (Japan), together with NRC (Canada) and NSC and ASIAA (Taiwan), in cooperation with the Republic of Chile. The Joint ALMA Observatory is operated by ESO, AUI/NRAO and NAOJ. This research is based in part on observations made with Herschel. Herschel is an ESA space observatory with science instruments provided by European-led Principal Investigator consortia and with important participation from NASA. This research makes use of data based on observations obtained at the Gemini Observatory, which is operated by the Association of Universities for Research in Astronomy, Inc., under a cooperative agreement with the NSF on behalf of the Gemini partnership: the National Science Foundation (United States), the National Research Council (Canada), CONICYT (Chile), the Australian Research Council (Australia), Ministério da Ciência, Tecnologia e Inovação (Brazil) and Ministerio de Ciencia, Tecnología e Innovación Productiva (Argentina).

Author Contributions

B.H. had the overall lead of the project. B.H. reduced the ALMA data and wrote the manuscript. K.O. conducted the photometry of the Gemini and Herschel data. All authors contributed to the ALMA proposal, discussed the results and implications, and commented on the manuscript.

Author Information

This research is based on the following ALMA data: ADS/JAO.ALMA#2011.0.00232.S. Reprints and permissions information is available at www.nature.com/reprints. The authors declare no competing financial interests. Correspondence and requests for materials should be addressed to B.H. (bunyo.hatsukade@nao.ac.jp)

Table 1 | Properties of GRB host galaxies

	GRB 020819B		GRB051022
	Nuclear region	GRB site	
z_{CO} ∗	0.410		0.806
CO transition	3–2		4–3
$L'_{\mathrm{CO(1-0)}}$ (K km s^{-1} pc^2) †	$(5.5 \pm 0.4) \times 10^8$	$<1.3 \times 10^8$	$(4.9 \pm 0.9) \times 10^9$
M_{gas} ($M_\odot$) ‡	$(2.4 \pm 0.2) \times 10^9$	$<5.4 \times 10^8$	$(2.1 \pm 0.4) \times 10^9$
$S_{1.2\ \mathrm{mm}}$ (mJy) §	<0.12	0.14 ± 0.03	0.10 ± 0.03
M_{dust} ($M_\odot$) ‖	$<4.2 \times 10^7$	$(4.8 \pm 1.0) \times 10^7$	$(2.9 \pm 0.9) \times 10^7$
L_{FIR} ($L_\odot$) ¶	$<9.3 \times 10^{10}$	$(1.1 \pm 0.2) \times 10^{11}$	$(1.9 \pm 0.6) \times 10^{11}$
SFR ($M_\odot$ yr^{-1}) #	<16	18 ± 4	32 ± 10
$M_{\mathrm{gas}}/M_{\mathrm{dust}}$	>51–60	<9–14	58–86

The errors represent root mean square (1σ) uncertainties from the photometry error. The limits are 3σ. We adopt a cosmology with $H_0 = 71$ km s^{-1} Mpc^{-1}, $\Omega_M = 0.27$, and $\Omega_\Lambda = 0.73$. For details, see Methods.

∗ Redshift determined from the CO line.

† CO(1–0) luminosity derived from $L'_{\mathrm{CO}} = 3.25 \times 10^7\ S_{\mathrm{CO}}\Delta v\, \nu_{\mathrm{obs}}^{-2} D_{\mathrm{L}}^2 (1+z)^{-3}$, where L'_{CO} in units of K km s^{-1} pc^2, $S_{\mathrm{CO}}\Delta v$ is the velocity-integrated flux in Jy km s^{-1}, ν_{obs} is the observed line frequency in GHz, D_{L} is the luminosity distance in Mpc. We assume a CO line ratio of CO(3–2)/CO(1–0) = 0.93 and CO(4–3)/CO(1–0) = 0.85, values for the local star-forming galaxy M82.

‡ Molecular gas mass derived from $M_{\mathrm{gas}} = \alpha_{\mathrm{CO}} L'_{\mathrm{CO(1-0)}}$, where α_{CO} is the CO-to-molecular gas mass conversion factor of a Galactic value $\alpha_{\mathrm{CO}} = 4.3$ in units of $M_{\odot}$ (K km s^{-1} $\mathrm{pc}^2)^{-1}$.

§ 1.2 mm continuum flux.

‖ Dust mass derived from $M_{\mathrm{dust}} = S_{\mathrm{obs}} D_{\mathrm{L}}^2 / [(1+z)\ \kappa_{\mathrm{d}}(\nu_{\mathrm{rest}}) B(\nu_{\mathrm{rest}}, T_{\mathrm{d}})]$, where S_{obs} is the observed flux density, ν_{rest} is the rest frequency, $\kappa_{\mathrm{d}}(\nu_{\mathrm{rest}})$ is the rest-frequency mass absorption coefficient , $B(\nu_{\mathrm{rest}}, T_{\mathrm{d}})$ is the Planck blackbody function.

¶ FIR luminosity derived from $L_{\mathrm{FIR}} = 4\pi M_{\mathrm{d}} \int_0^{\infty} \kappa_{\mathrm{d}}(\nu) B(\nu, T_{\mathrm{d}}) \mathrm{d}\nu$.

Star-formation rate derived from SFR (in $M_{\odot}$ yr^{-1}) = $1.72 \times 10^{-10}\ L_{\mathrm{FIR}}$ (in $L_{\odot}$).

Figure 1 | CO maps, 1.2 mm continuum maps, and optical images of the GRB hosts. Magenta crosses represent the position of radio afterglow. **a**, Velocity-integrated CO(3–2) intensity map. CO emission is detected at the nuclear region of the host. Contours are plotted at -3σ, 3σ, 5σ, 7σ, and 9σ (1σ = 0.40 Jy beam^{-1} km s^{-1}). The component size of the CO emission (deconvolved from beam) derived from a Gaussian fitting is 3.2 × 1.5 kpc (FWHM). The beam size (FWHM 0.8" × 0.7") is shown in the lower left. **b**, 1.2 mm continuum map obtained with a total bandwidth of ~7.5 GHz (excluding channels with emission line). Contours are plotted at -3σ, 3σ, and 4σ (1σ = 0.030 mJy beam^{-1}). The emission is detected at the explosion site of GRB 020819B, ~3" (16 kpc in projection) north from the nuclear region. **c**, Optical *R*-band image obtained with the Gemini North Telescope. **d**, Velocity-integrated CO(4–3) intensity map. Contours are plotted at 3σ, 4σ, and 5σ (1σ = 0.37 Jy beam^{-1} km s^{-1}). The beam size (FWHM 1.0" × 0.7") is shown in the lower left. **e**, 1.2 mm continuum map obtained with a total bandwidth of ~7.5 GHz (excluding channels with emission line). Contours are plotted at ±3σ (1σ = 0.032 mJy beam^{-1}). **f**, Optical *R*-band image obtained with the Gemini South Telescope.

Figure 2 | CO spectra of the GRB hosts. Continuum emission is subtracted. **a**, CO(3–2) spectrum of the nuclear region of the GRB 020819B host at 20 km s^{-1} resolution. A Gaussian fit to the emission line gives a redshift of $z = 0.410$ and a velocity width of 167 km s^{-1} (FWHM). **b**, CO(4–3) spectrum of the GRB 051022 host at 30 km s^{-1} resolution. A Gaussian fit to the emission line gives a redshift of $z = 0.806$ and a velocity width of 176 km s^{-1} (FWHM).

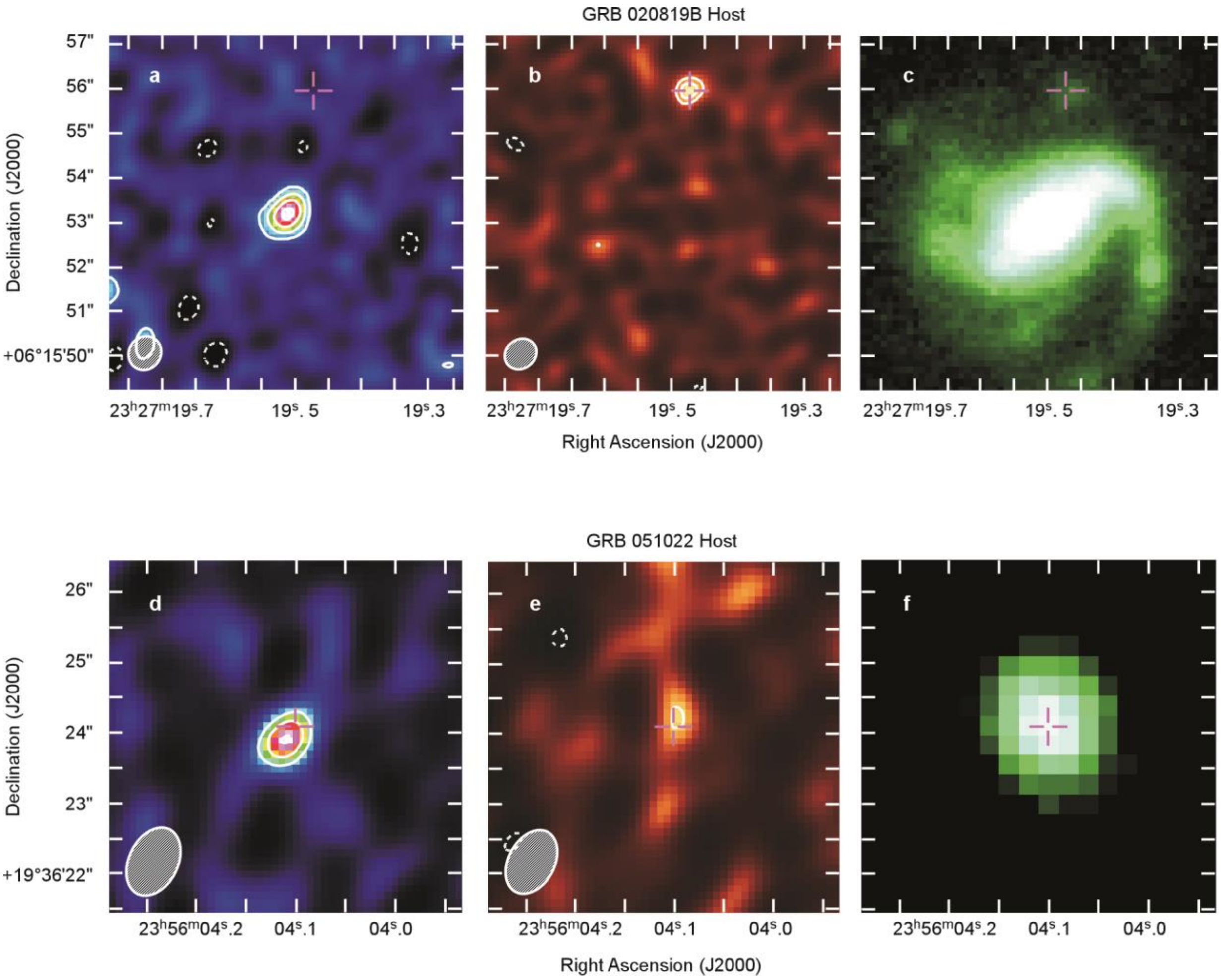
GRB 020819B Host
a
b
c
57"
56"
55"
54"
53"
52"
51"
+06°15'50"
Declination (J2000)
23h27m19s.7
19s.5
19s.3
Right Ascension (J2000)
GRB 051022 Host
d
e
f
26"
25"
24"
23"
+19°36'22"
Declination (J2000)
23h56m04s.2
04s.1
04s.0
Right Ascension (J2000)

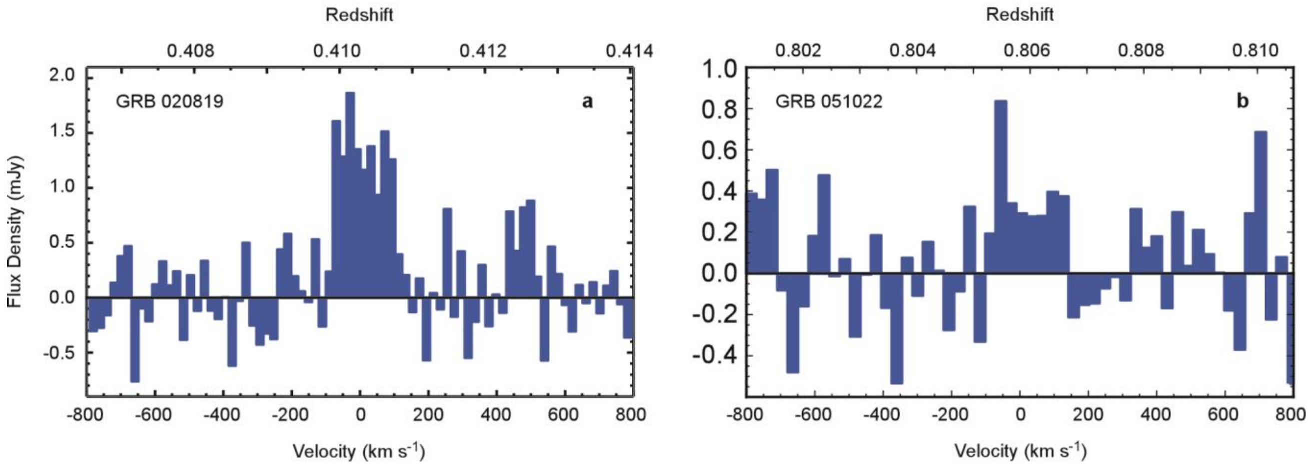
Redshift
0.408
0.410
0.412
0.414
GRB 020819
a
Flux Density (mJy)
2.0
1.5
1.0
0.5
0.0
-0.5
-800
-600
-400
-200
0
200
400
600
800
Velocity (km s-1)
Redshift
0.802
0.804
0.806
0.808
0.810
GRB 051022
b
1.0
0.8
0.6
0.4
0.2
0.0
-0.2
-0.4
-800
-600
-400
-200
0
200
400
600
800
Velocity (km s-1)

Methods Summary

We conducted ALMA observations of GRB 020819B host and GRB 051022 host at 245.072 GHz and 255.142 GHz, respectively, with a bandwidth of 1875 MHz and with 24-27 antennas. The data were reduced with the CASA package in a standard manner. The maps were processed with the CLEAN algorithm with Briggs weighting (robust = 0.5). The final synthesized beam size (FWHM) is ~0.8″ × 0.7″ and ~1.0″ × 0.7″ for the GRB 020819B host and the GRB 051022 host, respectively. We derived the molecular gas mass of $M_{\mathrm{gas}} = (2.4 \pm 0.2) \times 10^9\ M_{\odot}$ and $(2.1 \pm 0.4) \times 10^9\ M_{\odot}$ for the nuclear region of the GRB 020819B host and the GRB 051022 host, respectively. Here we assume CO line ratios of CO(3–2)/CO(1–0) = 0.93 and CO(4–3)/CO(1–0) = 0.85, values for the local star-forming galaxy M82, by considering the star-forming property of the hosts. We adopt the CO-to-molecular gas mass conversion of Galactic value ($4.3\ M_{\odot}\ (\mathrm{K\ km\ s^{-1}\ pc^{2}})^{-1}$) because the metallicity of the two hosts is close to the solar metallicity. To estimate a dust temperature and an emissivity index, we fitted a single temperature modified blackbody form to the FIR-millimetre photometry of the ALMA 1.2 mm data and *Herschel* 100 μm, 160 μm, and 250 μm data. The best-fit results are $T_{\mathrm{dust}} = 28 \pm 3$ K and $\beta = 1.9 \pm 0.3$ for the GRB 020819B host and $T_{\mathrm{dust}} = 34 \pm 6$ K and $\beta = 1.8 \pm 0.5$ for the GRB 051022 host. By using the best-fit modified blackbody functions, we derived dust mass of $(4.8 \pm 0.1) \times 10^7\ M_{\odot}$ and $(2.9 \pm 0.9) \times 10^7\ M_{\odot}$ for the GRB 020819B site and the GRB 051022 host, respectively.

Methods

Observations, data reduction, and results. We conducted ALMA band 6 observations of GRB 020819B host in 2012 November 17 with 27 antennas and GRB 051022 host in 2012 November 21 and December 2 with 24 antennas during the ALMA Cycle 0 session. The range of baseline lengths of the configuration is 15-402 m and 15-382 m for the observations of GRB 020819B host and GRB 051022 host, respectively. The maximum recoverable scale (the largest angular structure to which a given array is sensitive) for the array configurations is 10", which is large enough to cover the angular scale of the host galaxies. The correlator was used in the frequency domain mode with a bandwidth of 1875 MHz (488.28 kHz × 3840 channels). Four basebands were used, giving a total bandwidth of 7.5 GHz. We observed the redshifted CO(3–2) line at 245.072 GHz for the GRB 020819B host and the redshifted CO(4–3) line at 255.142 GHz for the GRB 051022 host. Uranus was observed as a flux calibrator and a quasar J2253+161 (3C454.3) was observed for bandpass and phase calibrations. The on-source time is xx min and 71 min for GRB 020819B host and GRB 051022 host, respectively. The data were reduced with the Common Astronomy Software Applications[31] package in a standard manner. The maps were processed with the CLEAN algorithm with Briggs weighting (robust = 0.5). The final synthesized beam size (FWHM) is ~0.8″ × 0.7″ and ~1.0″ × 0.7″ for the GRB 020819B host and the GRB 051022 host, respectively. CO emission and 1.2 mm continuum emission are detected at both GRB host galaxies (Figs. 1a, b, d, e, and 2). The GRB 020819B host is spatially resolved in the observations, while the GRB 051022 host is not. The velocity-integrated CO intensity is $S_{\mathrm{CO(3–2)}}$ = 0.53

± 0.04 Jy km s^{-1} and $S_{CO(4–3)}$ = 0.19 ± 0.03 Jy km s^{-1} at the nucleus of the GRB 020819B host and the GRB 051022 host, respectively. The 1.2 mm continuum flux density is $S_{1.2mm}$ = 0.14 ± 0.03 Jy and $S_{1.2mm}$ = 0.10 ± 0.03 Jy at the explosion site of GRB 020819B and the GRB 051022 host, respectively.

Molecular Gas Mass. CO luminosity is derived from $L'_{CO} = 3.25 \times 10^7\, S_{CO}\Delta v\, \nu_{obs}^{-2} D_L^2 (1+z)^{-3}$ (ref. 23), where L'_{CO} in units of K km s^{-1} pc^2, $S_{CO}\Delta v$ is the velocity-integrated flux in Jy km s^{-1}, ν_{obs} is the observed line frequency in GHz, and D_L is the luminosity distance in Mpc. We assume a CO line ratio of CO(3–2)/CO(1–0) = 0.93 and CO(4–3)/CO(1–0) = 0.85, values for the local star-forming galaxy M82 (ref. 32), by considering the star-forming property of the host galaxies. The derived CO(1–0) luminosity is $(5.5 \pm 0.4) \times 10^8$ (K km s^{-1} pc^2) and $(4.9 \pm 0.9) \times 10^9$ (K km s^{-1} pc^2) for the nuclear region of the GRB 020819B host and the GRB 051022 host, respectively. Molecular gas mass is derived from $M_{gas} = \alpha_{CO} L'_{CO(1–0)}$, where α_{CO} is the CO-to-molecular gas mass conversion factor in units of $M_\odot$ (K km s^{-1} $pc^2)^{-1}$ including He mass. It is thought that there is a correlation between α_{CO} and metallicity in the local universe and at $z \sim 1–2$ (refs. 33,34); α_{CO} decreases with increasing metallicity. Because the metallicity of the two hosts is close to the solar metallicity, we adopt α_{CO} of Galactic value of α_{CO} = 4.3 $M_\odot$ (K km s^{-1} $pc^2)^{-1}$ (ref. 35). The derived molecular gas mass is $M_{gas} = (2.4 \pm 0.2) \times 10^9\, M_\odot$ and $(2.1 \pm 0.4) \times 10^9\, M_\odot$ for the nuclear region of the GRB 020819B host and the GRB 051022 host, respectively.

Photometry of *Herschel* Space Observatory[36] data. We used the *Herschel*/Photodetector Array Camera and Spectrometer (PACS)[37] data in the archive. We conducted aperture photometry on the 160 μm image of the GRB 051022 host with SExtractor[38] and obtained the flux density of $S_{160\,\mu\mathrm{m}} = 12$ mJy (with about 30% photometry error). There is no significant contamination from nearby sources to the photometry. The FWHMs of the source size is ~14″ at 160 μm, respectively, which is comparable to the FWHM of PACS beam size[37]. We also measured the centroid of the 100 μm emission of the GRB 020819B host and found that the emission is in between the galaxy centre and the peak of 1.2 mm continuum. It is possible that dust is more widely spread in the host galaxy, although the angular resolution is inadequate (FHWM of ~7″).

Modified blackbody fit. To estimate a dust temperature (T_{dust}) and an emissivity index (β), we fitted the FIR-millimetre photometry data of *Herschel* 100 μm, 160 μm, and 250 μm (ref. 9), and ALMA 1.2 mm with a single temperature modified blackbody form of $S_\nu \propto \nu^{3+\beta}/(\exp(h\nu/kT_{\mathrm{dust}})-1)$, where S_ν is the flux density and ν is the frequency. The best-fit results are $T_{\mathrm{dust}} = 28 \pm 3$ K and $\beta = 1.9 \pm 0.3$ for the GRB 020819B host and $T_{\mathrm{dust}} = 34 \pm 6$ K and $\beta = 1.8 \pm 0.5$ for the GRB 051022 host. We note that the missing flux in the ALMA observations in the scale of the PACS beamsize is negligible. The dust temperatures are within the typical range of $z \sim 0$–2 star-forming galaxies[39,40]. Dust temperatures of the hosts were derived in a previous study with SED model fit to optical-IR data including *Herschel* photometry[9]: $T_{\mathrm{dust}} = 24.4$ K and 52.6 K for the GRB 020819B host and the GRB 051022 host, respectively. The dust temperature of the GRB 051022 host is higher than our work. This may be due to the lack of their photometric data at >160 μm, which is essential to fit dust SED.

Dust mass, FIR luminosity, and SFR. By using the best-fit modified blackbody functions, we estimated dust mass, FIR luminosity, and SFR. Dust mass is derived by $M_{\mathrm{dust}} = S_{\mathrm{obs}}D_{\mathrm{L}}^2/[(1+z)\,\kappa_{\mathrm{d}}(\nu_{\mathrm{rest}})B(\nu_{\mathrm{rest}}, T_{\mathrm{dust}})]$ (ref. 45), where S_{obs} is the observed flux density, ν_{rest} is the rest frequency, $\kappa_{\mathrm{d}}(\nu_{\mathrm{rest}})$ is the rest-frequency mass absorption coefficient, $B(\nu_{\mathrm{rest}}, T_{\mathrm{dust}})$ is the Planck function. We assume that the absorption coefficient varies as $\kappa_{\mathrm{d}}(\nu) \propto \nu^{\beta}$ and $\kappa_{\mathrm{d}}(125\ \mu\mathrm{m}) = 26.4\ \mathrm{cm}^2\ \mathrm{g}^{-1}$ (ref. 46). The derived dust mass is $(4.8 \pm 0.1) \times 10^7\ M_{\odot}$ and $(2.9 \pm 0.9) \times 10^7\ M_{\odot}$ for the GRB 020819B site and the GRB 051022 host, respectively. If we use the dust temperature of 52.6 K for the GRB 051022 host estimated in a previous work[9], the derived dust mass would be about a factor of two lower, which has no effect on the discussion in the main text. FIR luminosity is derived from $L_{\mathrm{FIR}} = 4\pi M_{\mathrm{dust}} \int_0^{\infty} \kappa_{\mathrm{d}}(\nu)B(\nu, T_{\mathrm{dust}})d\nu$ (ref. 45). The derived FIR luminosity is $(1.1 \pm 0.2) \times 10^{11}\ L_{\odot}$ and $(1.9 \pm 0.6) \times 10^{11}\ L_{\odot}$ for the GRB 020819B site and the GRB 051022 host, respectively. SFR is derived from the FIR luminosity as SFR (in $M_{\odot}\ \mathrm{yr}^{-1}$) $= 1.72 \times 10^{-10}\ L_{\mathrm{FIR}}$ (in $L_{\odot}$) (ref. 47), and calculated to be $18 \pm 4\ M_{\odot}\ \mathrm{yr}^{-1}$ and $32 \pm 10\ M_{\odot}\ \mathrm{yr}^{-1}$ for the GRB 020819B site and the GRB 051022 host, respectively.

31. McMullin, J. P. *et al*. CASA architecture and applications. *ASP Conf. Ser. 376, Astronomical Data Analysis Software and Systems XVI, ed. R. A. Shaw, F. Hill, & D. J. Bell (San Francisco, CA: ASP)*, 127–130 (2007)

32. Carilli, C. L., & Walter, F. Cool gas in high-redshift galaxies. *Annu. Rev. Astron. Astrophys.* **51**, 105–161 (2013)

33. Wilson, C. D. The metallicity dependence of the CO-to-H_2 conversion factor from observations

of local group galaxies. *Astrophys. J.* **448**, L97–L100 (1995)

34. Genzel, R. *et al*. The metallicity dependence of the CO → H_2 conversion factor in $z \geq 1$ star-forming galaxies. *Astrophys. J.* **746**, 69–79 (2012)
35. Bolatto, A. D., Wolfire, M., & Leroy, A. K. The CO-to-H2 conversion factor. *Annu. Rev. Astron. Astrophys.* **51**, 207–268 (2013)
36. Pilbratt, G. L. *et al. Herschel* Space Observatory. An ESA facility for far-infrared and submillimetre astronomy. *Astron. Astrophys.* **518**, L1 (2010)
37. Poglitsch, A. *et al.* The Photodetector Array Camera and Spectrometer (PACS) on the *Herschel* Space Observatory. *Astron. Astrophys.* **518**, L2 (2010)
38. Bertin, E., & Arnouts, S. SExtractor: Software for source extraction. *Astron. Astrophys. Suppl.* **117**, 393–404 (1996)
39. Elbaz, D. *et al.* GOODS-Herschel: an infrared main sequence for star-forming galaxies. *Astron. Astrophys.* **533**, 119–144 (2011)
40. Symeonidis, M. *et al*. The Herschel census of infrared SEDs through cosmic time. *Mon. Not. R. Astron. Soc.* **431**, 2317–2340 (2013)
41. Silva, L. *et al*. Modeling the effects of dust on galactic spectral energy distributions from the ultraviolet to the millimeter band. *Astrophys. J.* **509**, 103–117 (1998)

42. Svensson, K. M., Levan, A. J., Tanvir, N. R., Fruchter, A. S., & Strolger, L.-G. The host galaxies of core-collapse supernovae and gamma-ray bursts. *Mon. Not. R. Astron. Soc.* **405**, 57–76 (2010)

43. Stanway, E. R., Davies, L. J. M., & Levan, A. J. Low radio-derived star formation rates in $z < 0.5$ gamma-ray burst host galaxies. *Mon. Not. R. Astron. Soc.* **409**, L74–L78 (2010)

44. Hatsukade, B. *et al*. Constraints on obscured star formation in host galaxies of gamma-ray bursts. *Astrophys. J.* **748**, 108–111 (2012)

45. De Breuck, C. *et al.* CO emission and associated HI absorption from a massive gas reservoir surrounding the $z = 3$ radio galaxy B3 J2330+3927. *Astron. Astrophys.* **401**, 911–925 (2003)

46. Dunne, L. *et al.* A census of metals at high and low redshift and the connection between submillimetre sources and spheroid formation. *Mon. Not. R. Astron. Soc.* **341**, 589–598 (2003)

47. Kennicutt, R. C., Jr. The global Schmidt law in star-forming galaxies. *Astrophys. J.* **498**, 541–552 (1998)

48. Le Floc'h, E. *et al.* Probing cosmic star formation using long gamma-ray bursts: new constraints from the *Spitzer Space Telescope*. *Astrophys. J.* **642**, 636–652 (2006)

49. Michałowski, M. J. *et al*. The properties of the host galaxy and the immediate environment of GRB 980425/SN 1998bw from the multiwavelength spectral energy distribution. *Astrophys. J.* **693**, 347–354 (2009)

50. Michałowski, M. J. *et al.* Spatially-resolved dust properties of the GRB 980425 host galaxy. *Astron. Astrophys.* **562**, A70–82 (2014)

51. Hatsukade, B. *et al*. Faint end of 1.3 mm number counts revealed by ALMA. *Astrophys. J.* **769**, L27–L31 (2013)

52. Daddi, E. *et al.* Very high gas fractions and extended gas reservoirs in z = 1.5 disk galaxies. *Astrophys. J.* **713**, 686–707 (2010)

53. Gao, Y., & Solomon, P. M. The star formation rate and dense molecular gas in galaxies. *Astrophys. J.* **606**, 271–290 (2004)

54. Combes, F. *et al.* Galaxy evolution and star formation efficiency at $0.2 < z < 0.6$. *Astron. Astrophys.* **528**, 124–134 (2011)

55. Combes, F. *et al.* Gas fraction and star formation efficiency at $z < 1.0$. *Astron. Astrophys.* **550**, 41–55 (2013)

Extended Data Figure 1 | Spectral energy distribution of GRB 020819B host and GRB 051022 host. The red squares show ALMA 1.2 mm data. Black squares represent photometry from literatures[10,11,14,24,42,43,44] and archive data. Dashed curves show the best-fit modified blackbody functions. The arrows represent 3σ upper limits. For comparison, we plot SED models of Arp220, M82, NGC6946, and M51 (ref. 41). The SED models are scaled to the flux density of ALMA data.

Extended Data Figure 2 | Comparison of CO and FIR luminosities. The GRB 020819B host and the GRB 051022 host are plotted with 1σ uncertainties (red and blue squares). The error bars are from 1σ uncertainty. Various galaxy populations are also plotted: local spirals[20,53] (circles), local LIRGs (plus) and ULIRGs[23,53] (x), $z \sim 0.2$–1 ULIRGs[54,55] (diamonds), $z \sim 1$–2 normal star-forming galaxies[21] (pentagons), SMGs[22,23] (up-pointing triangles), QSOs and radio galaxies[23] (down-pointing triangles). Grey solid and dashed lines represent the sequence of normal star-forming galaxies and starburst galaxies, respectively[52].

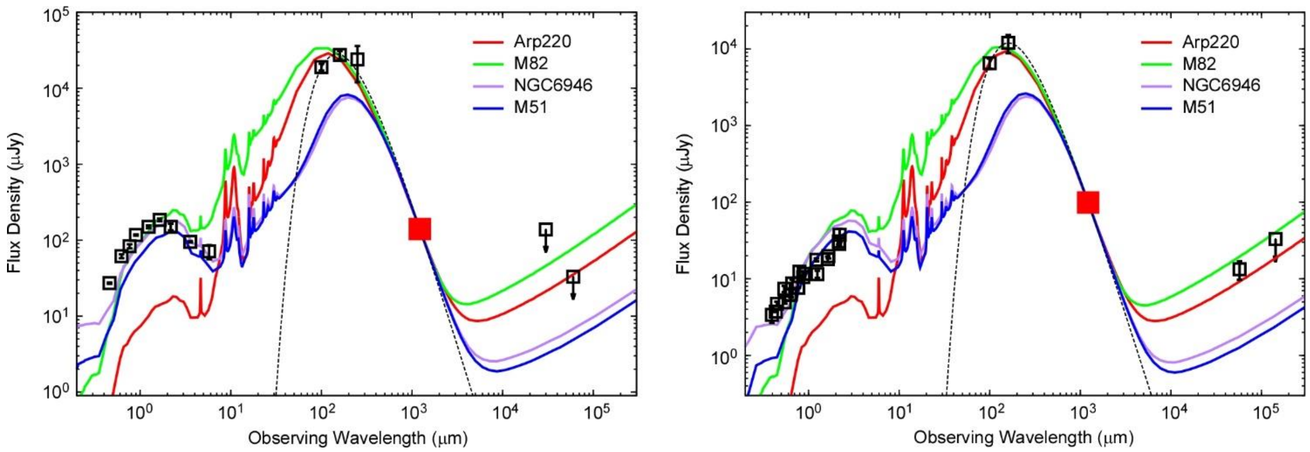
Flux Density (μJy)
Observing Wavelength (μm)
Arp220
M82
NGC6946
M51
10^0
10^1
10^2
10^3
10^4
10^5
Flux Density (μJy)
Observing Wavelength (μm)
Arp220
M82
NGC6946
M51
10^0
10^1
10^2
10^3
10^4
10^5

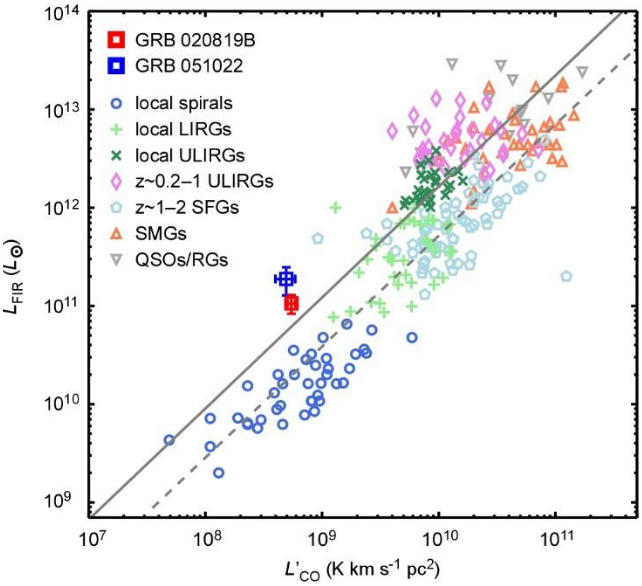
GRB 020819B
GRB 051022
local spirals
local LIRGs
local ULIRGs
z~0.2–1 ULIRGs
z~1–2 SFGs
SMGs
QSOs/RGs
$L_{\rm FIR}$ ($L_\odot$)
$L'_{\rm CO}$ (K km s^{-1} pc^2)
10^9
10^{10}
10^{11}
10^{12}
10^{13}
10^{14}
10^7
10^8
10^9
10^{10}
10^{11}

Supplementary Information

Spectral Energy Distribution

We created spectral energy distributions (SEDs) of the host galaxies of GRB 020819B and GRB 051022 from optical to radio wavelength by using photometry data of our ALMA observations, the archive data of *Herschel*, and literatures. We plot the SEDs of the GRB 020819B host and GRB 051022 host in Extended Data Fig. 1. For comparison, we show the SED models[41] of local galaxies Arp220 (archetypal ultra-luminous IR galaxies; ULIRGs), M82 (prototype starburst), NGC6946, and M51 (spiral galaxies). The SED models are redshifted to each host galaxy and normalized to the flux density of ALMA observations. The SEDs of both GRB hosts are closer to starburst galaxies than spiral galaxies.

Origin of the Continuum Emission in the GRB 020819B Host Galaxy

The 1.2 mm continuum emission in the GRB 020819B host galaxy is only detected at the position of the GRB site. A similar case is reported in the host galaxy of GRB 980425, where a star-forming region ~800 pc away from the GRB site dominates the IR emission of the entire host[48,49,50] The ALMA 1.2 mm photometry data is well explained by the modified blackbody spectrum (Extended Data Fig. 1) and the inferred SFR is comparable to the extinction-corrected SFR derived from UV and optical observations. These suggest that the origin of the continuum emission at the GRB is most likely the dust thermal emission heated by star-forming activity in the host galaxy. Nevertheless, we discuss alternative possibilities for the origin of the 1.2 mm emission below: (1) emission from other galaxy behind the host, and (2) synchrotron emission from the GRB remnant.

(1) The peak position of the 1.2 mm continuum emission is α(J2000.0) = $23^h27^m19^s.47$ and δ(J2000.0) = 06°15′55″.95. The positional uncertainty for a SN = 4.7 source is ~0.17″. The 1.4 GHz radio afterglow position is α(J2000) = $23^h27^m19^s.475$ and δ(J2000) = 06°15′55″.95, with an error of 0″.5 (ref. 13). The positional offset between them is 0″.06, which is sufficiently small compared to the positional uncertainty. We estimate the probability that a source behind the host galaxy is coincidentally detected at the GRB position. The spatial density of sources with $S_{1.2\mathrm{mm}} \geq 0.14$ is $\sim 3 \times 10^4$ deg^{-2} based on the recently obtained number counts at 1.3 mm (ref.51). The expected number of sources which fall within a radius of 0″.06 is $\sim 3 \times 10^{-5}$. The chance coincident is significantly small and we can conclude that the 1.2 mm continuum emission comes from the GRB site.

(2) The radio continuum observations of the GRB 020819B host at 3 cm and 6 cm in January 2010 did not detect emission, giving the 3σ upper limits of $S_{3\mathrm{cm}} < 138$ μJy and $S_{6\mathrm{cm}} < 33$ μJy (ref.43). Because the spectral index of synchrotron emission against the wavelength is positive, the upper limits reject the possibility that the 1.2 mm continuum emission is attributed to synchrotron emission.

Considering the above, we can regard the continuum emission as dust thermal emission originated in star-forming activity. We note that there is a possibility that the dust was heated by the GRB explosion. However, we do not consider this possibility here because many uncertainties remain (e.g., the amount of dust, the dusty geometry, how much of the explosion energy is transferred to dust heating).

Comparison of CO and FIR Luminosities

Recent molecular gas observations of local and high-redshift star-forming galaxies suggest the existence of two different star-formation modes[52]: (1) long-lasting mode for disks seen in local spirals and $z \sim 1$–2 normal star-forming galaxies, and (2) more rapid mode for starburst galaxies seen in local ULIRGs and SMGs. It is proposed that the two types of galaxies are located in separate sequences in L'_{CO}–L_{FIR} plane (Extended Data Fig. 2). In order to examine the properties of the GRB host galaxies as a whole and to compare with previous studies, we plot our data without separating the nuclear region and the explosion site for the GRB 020819B host. The two GRB hosts are closer to the sequence for starburst galaxies, suggesting that the star-forming activity in the hosts has property of starburst galaxies.